Data supplement for Girault et al., Infant Visual Brain Development and inherited Genetic Liability in Autism. Am J Psychiatry (doi: 10.1176/appi.ajp.21101002)

SUPPLEMENTARY METHODS

Participants

All participants were screened and excluded based on the following criteria: known genetic conditions or syndromes in the proband or infant, medical/neurological conditions affecting growth, development, or cognition (e.g., vision or hearing loss), birth weight <2000g and/or gestational age <36 weeks or significant perinatal adversity and/or exposure to in utero neurotoxins, contraindication for MRI, predominant home language other than English, adopted children or half siblings, first-degree relative with psychosis, schizophrenia, or bipolar disorder screened using the Family Interview for Genetic Studies, and multiple gestation pregnancy.

Of the 414 participants who were followed to outcome at 24 months and received DSM diagnostic classifications, 14 participants were removed owing to missing proband behavioral data, four participants were removed due to meeting exclusion criteria after enrollment (identified genetic syndrome in the proband (n = 2), medical complication identified in the proband prior to onset of ASD (n = 2)), and 12 participants were removed because they were biological siblings of another high-risk sibling in the cohort (i.e. more than one younger sibling was recruited from the same family). In the case of related high-risk siblings, the sibling with the most available data (neuroimaging data at 6, 12, and 24 months) was selected for inclusion in the study; the selection was made blinded to the diagnostic outcome of the child. A total of 384 proband-sibling pairs were included in the present study (**Table S1**), 89 of whom were concordant for a diagnosis of ASD, meaning the younger sibling received a diagnosis of ASD at 24 months of age.

Imaging Procedures

The imaging protocol included a localizer scan, 3D T1 MPRAGE (TR = 2,400ms, TE = 3.16ms, 160 sagittal slices, FOV = 256mm, voxel size = $1mm^3$), 3D T2 TSE (TR = 3,200ms, TE = 499ms, 160 sagittal slices, FOV = 256mm, voxel size = $1mm^3$), and a 25-direction diffusion weighted imaging (DWI) sequence. The DWI sequence was an ep2d_diff pulse sequence with a FOV of 190mm (6 and 12 months) or 206mm (24 months), 75-81 transversal slices, and voxel size of $2mm^3$, TR = 12,800-13,300ms, TE=102ms, with 26 DWI volumes with *b* values between 0 and 1,000s/mm^2 in increments of 40, including a single *b* = 0s/mm^2, and 25 gradient directions. The BOLD data were collected using gradient-echo echo planar image acquisition (TE = 27 ms; TR = 2500 ms; voxel size 4 x 4 x 4 mm^3). A minimum of two runs of 130 frames were required for inclusion. A number of quality control procedures were employed to assess scanner stability and reliability across sites, time, and procedures. Geometric phantoms were scanned monthly

and human phantoms (two adult subjects) were scanned annually to monitor scanner stability at each site across the study period. Details on the stability procedures and quality control checks are described elsewhere(1, 2). All scans underwent radiological review by a licensed neuroradiologist(1); no subjects included in this report had clinically significant abnormalities on any MRI at any age. MRI sample sizes by age are shown **Table S2**.

Image Analysis

Image processing was performed to obtain global brain tissue volumes, global and regional cortical surface area measurements, extra-axial cerebrospinal fluid volumes, and tract-based measures of white matter integrity. All image processing and quality control was conducted blind to the subject diagnostic information.

Brain volumes were obtained using a framework of atlas-moderated expectation maximization including co-registration of multi-modal (T1/T2) MRI, bias correction, brain masking, noise reduction, and multivariate classification with the AutoSeg toolkit (http://nitrc.org/projects/autoseg)(3). Population average templates and corresponding probabilistic brain tissue priors for white matter (WM), gray matter (GM), and cerebrospinal fluid (CSF) were constructed for the 6 to 24-month-old brain. The brain measure of interest included in this study is total cerebral volume, defined at the combined GM and WM volume of the cerebrum, including a segment of the midbrain and brainstem.

Cortical surface area measurements for 12 and 24-month images were obtained via a CIVET workflow adapted for pediatric images and using an age-corrected automated anatomical labeling (AAL) atlas(4, 5). CIVET uses shrink-wrap deformable surface evolution of WM, local Laplacian distance and local surface area, mapping to a spherical domain, co-registration using cortical sulcal features and extraction of regional measurements through a deformably co-registered fine-scale lobar parcellation. Surface area is computed along the geometric mid-cortical surface. For 6-month data sets, measurements were extracted from surfaces propagated via deformable multi-modal, within-subject co-registration(5) of MRI data sets from the 12-month scan. For this study, we utilized total surface area (TSA) measurements and as well as surface area measurements in targeted regions of interest (ROIs). These ROIs included those shown in Hazlett et al.(1) to be hyper-expanding in infants who develop ASD: right middle frontal gyrus, bilateral cuneus, right lingual gyrus, bilateral middle occipital gyrus, and left inferior temporal gyrus. To speak to the specificity of findings, two bilateral control ROIs were selected a-priori to not overlap with any ROIs shown to have differential development in infants who do develop ASD versus those who do not, or any ROIs shown to contribute to a prediction of ASD (see Figures 2 and 3 from Hazlett et al.,(1)). Selected control ROIs were the bilateral precentral gyrus (frontal lobe) and bilateral supramarginal gyrus (parietal lobe). Surface area ROIs are depicted in **Figure 2** in the main text.

Extra-axial CSF (EA-CSF) volumes were generated from a multi-modal (T1/T2) pipeline involving distortion correction, mutual registration, transformation to stereotactic space, and CSF/brain tissue segmentation(6). All images were corrected for geometric distortions and

intensity non-uniformity(7). T2 images were then registered to T1 images using mutual information registrations(8), and both co-registered images were transformed to stereotactic space. The skull was removed using a majority voting approach between T1, T2 and T1/T2 brain masks using FSL Brain Extraction Tool (BET)(9). Visual quality control confirmed only skull was removed. All corrected and skull-stripped T1 and T2 images were input into tissue segmentation pipeline to obtain GM, WM, and CSF(10). A deformable registration was used to map each subject-specific image to two study-specific atlas templates (6 and 12-24 month), and the lateral, third and fourth ventricles and cisterns were masked in atlas space and propagated to subject space to isolate CSF in the subarachnoid space. A ventral boundary at the horizontal plane of the anterior-posterior commissure was defined and the volume of EA-CSF surrounding the dorsolateral convexities of the cortical surface was measured.

Diffusion weighted images (DWIs) were pre-processed for appropriate quality using DTI prep(11). Visual quality control was performed by expert raters to remove additional images with residual artifacts. Data sets containing fewer than 18 of 25 total (72%) gradient directions after this two-step procedure were excluded from further processing to ensure consistent signal-to-noise ratio. As described in Wolff et al., approximately 10.5% of all acquired DTI data sets were excluded following quality control(12). Tractography was performed using the UNC-Utah NA-MIC framework(13) (www.nitrc.org/projects/namicdtifiber) using a study-specific template in 3D Slicer (www.slicer.org). Fractional anisotropy (FA) values were computed and averaged across each fiber tract, and tract-average values from a-priori selected fibers (splenium, and control tracts (genu, and body of the corpus callosum)) were used for analyses.

The functional MRI data were processed following methods described in previous IBIS publications(14, 15) using the 4dfp suite of tools (http://4dfp.readthedocs.io). Images were compensated for slice-dependent time shifts; head movement was quantified for spatial realignment both within and across runs; whole brain image intensity was normalized to a mode value of 1000(16); and images were registered into standardized 3-mm isotropic atlas space through an affine transformation. Processing for functional connectivity MRI applied global signal regression, nuisance signal regression, spatial and temporal bandpass filtering, and motion scrubbing(17). Motion scrubbing was implemented at a frame-to-frame displacement (FD) of 0.2 mm(18). To pass quality control, subjects must have a minimum of 6.25-minutes of scrubbed fcMRI; all infants included in this analysis provided a minimum of 7 minutes of scrubbed fcMRI (mean = 10.45min, SD = 2.5m).

The derivation and computation of time series data follow similar procedures as described previously for a primary set of 230 regions of interest (ROIs; 10-mm-diameter, spherical)(19), and ROI details are provided in the **Extended Data Table** (supplementary Excel file). In addition to the primary 230-ROI set, we generated (Hawks et al., under review) four new cerebellar ROIs by reverse-seeding frontoparietal and default mode networks(20–22). Functional connectivity values were calculated as Pearson correlations between pairs of ROI time-series and Fisher *r*-to-Z transformed for analyses. The full set of 234 ROIs were sorted into functional networks by applying the Infomap community detection algorithm(23) at edge densities ranging

from 0.02 to 0.10 (steps of 0.01). An automated procedure was used to generate a single consensus model of network structure, and structure-specific thresholding was used to integrate subcortical and cerebellar ROIs into whole-brain networks(24). Unassigned ROIs (n = 4) were excluded from network analyses. The network solution is shown below in **Figure S2**. Infant network nomenclature largely reflects naming of canonical networks found in adults; some network structures, however, appear to be specific to infants (e.g. pDMN was named as such because it contains the PCC, the adult DMN does not fracture into anterior and posterior components).

Statistical Analysis

Pearson correlations and confidence intervals were computed between proband SCQ score and each sibling global phenotype of interest to generate interpretable effect sizes. Correlations were computed separately for HR infants who received a diagnosis of ASD (ASD group) and those who did not (non-ASD group) at each of the visit time points (6, 12, and 24 months). *P*-values were adjusted using false discovery rate (FDR)(25) within each sibling group (ASD vs non-ASD) separately for global (cerebral volume, total surface area, EA-CSF volumes) and regional phenotypes (regional surface area, white matter FA in fiber tracts of interest). Brain phenotypes shown to exhibit significant correlations with proband SCQ scores (for global phenotypes $q < 0.05$, for regional phenotypes $P < 0.05$) were carried forward for further investigation. A slightly less strict selection was applied for regional phenotypes given the novelty of the study and a priori nature of the analysis.

Longitudinal mixed effects models for repeated measures were employed to analyze associations between proband SCQ score and sibling brain phenotypes from 6 to 24 months identified through Pearson correlation analyses above. Each brain phenotype was modeled separately, with a subject-specific intercept and slope. Fixed effects included proband SCQ score, sibling diagnosis, sibling age, sibling sex, and study site. Interaction terms between sibling diagnosis and proband SCQ score, and sibling diagnosis and age were also modeled. An unstructured covariance matrix was specified for the random effects while within-subject residuals were assumed to be independent. Mathematically, this model can be expressed as

$$Y_{ij} = \beta_0 + \beta_1 SCQ_{ij} + \beta_2 ASD_{ij} + \beta_3 Age_{ij} + \beta_4 Sex_{ij} + \beta_5 Site_{ij} + \beta_6 SCQ_{ij} * ASD_{ij} + \beta_7 Age_{ij} * ASD_{ij} + \varphi_{1i} + \varphi_{2i} * Age_{ij} + \varepsilon_{ij}$$

with i denoting subject and j denoting visit, φ denoting random effects, ε denoting residuals, and ASD, Sex, and Site being dummy-coded categorical variables. In secondary analyses, potential time-varying associations (e.g., splenium FA) were modeled with a three-way interaction term (proband SCQ score x sibling diagnosis x time). Model diagnostics were carried out visually to the primary models of interest by assessing the normalized conditional residuals for normality and homoscedasticity(26). Only one model was found to have non-normal residuals (total cerebral volume), this was mitigated by the large sample, resulting in asymptotically valid tests by the

central limit theorem(27). In sensitivity analyses, we included proband age and sex as covariates in our mixed models predicting brain phenotypes; we found that proband age and sex were not significant predictors of any sibling brain phenotype, consistent with our prior report finding no link between proband age and sex and sibling diagnostic outcomes or behavioral abilities(28), and thus the more parsimonious models (excluding proband age and sex) are reported.

To aid in the interpretation of effect size and visualization of data longitudinally, we dichotomized proband SCQ scores using a median split informed by evidence that proband SCQ scores in the upper quartiles conferred significantly increased risk for autism in infant siblings(28). For brain phenotypes significantly associated with proband SCQ score in mixed model analyses, least squares means were generated for the ASD group split by proband SCQ group (above vs. below the median SCQ; SCQ-High, SCQ-Low) and plotted across time. Percent differences in model-adjusted brain phenotypes at each time point and adjusted Cohen's *d* effect sizes were computed for ASD infants based on proband SCQ group. Additionally, to assess the generalizability of our results beyond a single parent report measure of ASD traits (SCQ), we also computed correlations using proband behavior derived from the Autism Diagnostic Interview-Revised (ADI-R), administered to a parent by a clinical expert(29). We tested two domain scores from the ADI-R with varying degrees of construct overlap and correlation with the proband SCQ: reciprocal social interaction (RSI; $r_{331} = 0.56$, $P < 0.0001$) and restricted and repetitive behaviors ($r_{331} = 0.19$, $P < 0.001$). Statistical analyses of structural and diffusion data were conducted using the R computing software, version 4.0.2 (2020).

Results from *a priori* analyses above led us to utilize our fcMRI data on a subset of our sample to test for associations between proband ASD traits and sibling functional connectivity at 6 months of age. Based on our other findings, we hypothesized that connections within and between visual networks would be associated with proband severity. If our hypotheses were correct, this would suggest multimodal anatomical and functional convergence on cortical regions, fiber pathways, and functional networks involved in visual processing. Rather than test visual circuitry directly, which could lead to confirmation bias, we conducted fcMRI enrichment analyses. Enrichment is a whole-brain approach (and therefore unbiased and data-driven) that identifies clusters of strong brain-behavior relationships within and between functional networks(14). Enrichment analyses were conducted using the 58 siblings ($n = 13$ ASD) with available fcMRI data at 6 months of age. The fcMRI data set is smaller than the structural and diffusion data sets due to a later onset of data collection during the course of the study. Owing to the limited number of subjects with fcMRI data available at 6 months of age, enrichment analyses were conducted across the *combined* sample (i.e., ASD and non-ASD), as in our prior published fcMRI work(14). This approach aligns with findings that functional connectivity did not differentiate infants based on diagnosis in cohort of a similar size (30).

Enrichment analyses were performed separately with the proband SCQ, ADI-R RSI, and VABS Socialization (VABS-Soc) scores. The VABS-Soc provides a complementary measure of social behavior available for a subset of probands. We used all three proband scores as inputs to our data-driven enrichment analysis to increase the search space. Analyses proceeded in three

steps, improving upon our prior fcMRI publications(14, 31) by accounting for familywise error rate with respect to the number of network pairs tested. First, the strongest 5% of sibling brain-proband behavior associations (*hits*) were identified in real and shuffled outcome (n = 50,000) data using mass univariate screening based on Spearman correlations. Second, for every network-network pair, enrichment P-values were computed as the fraction of shuffled runs with at least as many hits as real data. Based on simulations, it was determined that P-values < .001 were necessary to maintain 5% experiment-wide false-positive rate. To avoid overlooking potentially informative results given the novelty of the method and application, P-values < .01 were interpreted in the context of results from other imaging modalities. Python version 3.6.8 (2018) and MATLAB version 8.5 (2015a) were used to run enrichment analyses and generate figures.

Data Availability

Raw neuroimaging and behavioral data for infants in this study are publicly available at the National Institutes of Mental Health Data Archive (https://nda.nih.gov) in collections 0019 and 2027. Statistical code used to generate structural and diffusion imaging results is available via Github at https://github.com/kmdono02/Proband_Sibling_Brain_Imaging_Analysis. Code for fcMRI enrichment analyses is available via Github at https://github.com/CPD-Lab/ProbandEA.

SUPPLEMENTARY FIGURES AND TABLES

FIGURE S1. Infant Functional Network Solution

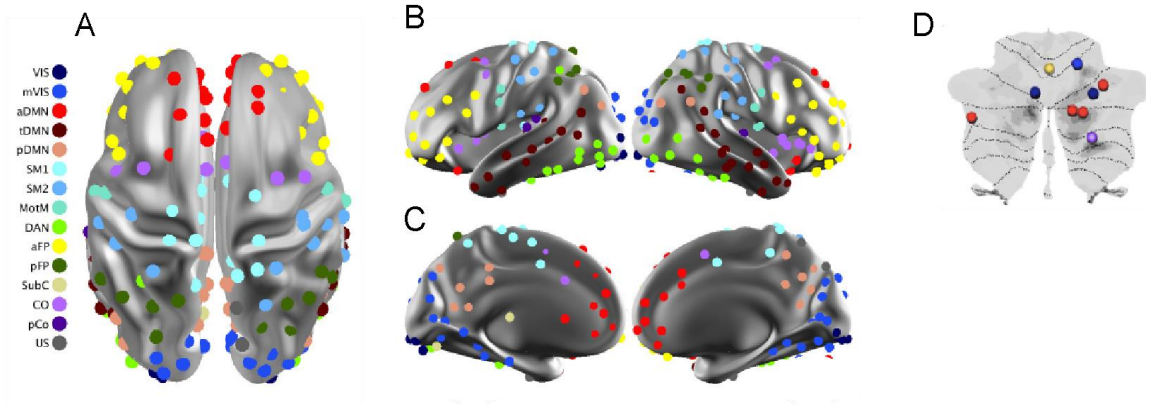

Infomap-derived functional networks are visualized on the (A) dorsal, (B) lateral, (C) medial, and (D) cerebellar surfaces. Network abbreviations are shown in (A): VIS = visual, mVIS = medial visual, aDMN = anterior default mode network, tDMN = temporal DMN, p = posterior DMN, SM1 = somato-motor 1, SM2 = somato-motor 2, MotM = mouth motor, DAN = dorsal attention network, aFP = anterior frontoparietal network, pFP = posterior FP, SubC = subcortical, CO = cingulo-opercular, pCO = posterior CO, US = unassigned

FIGURE S2. Trajectories of Right Middle Occipital Surface Area Differ Among ASD Infants Based on Proband ASD Trait Level

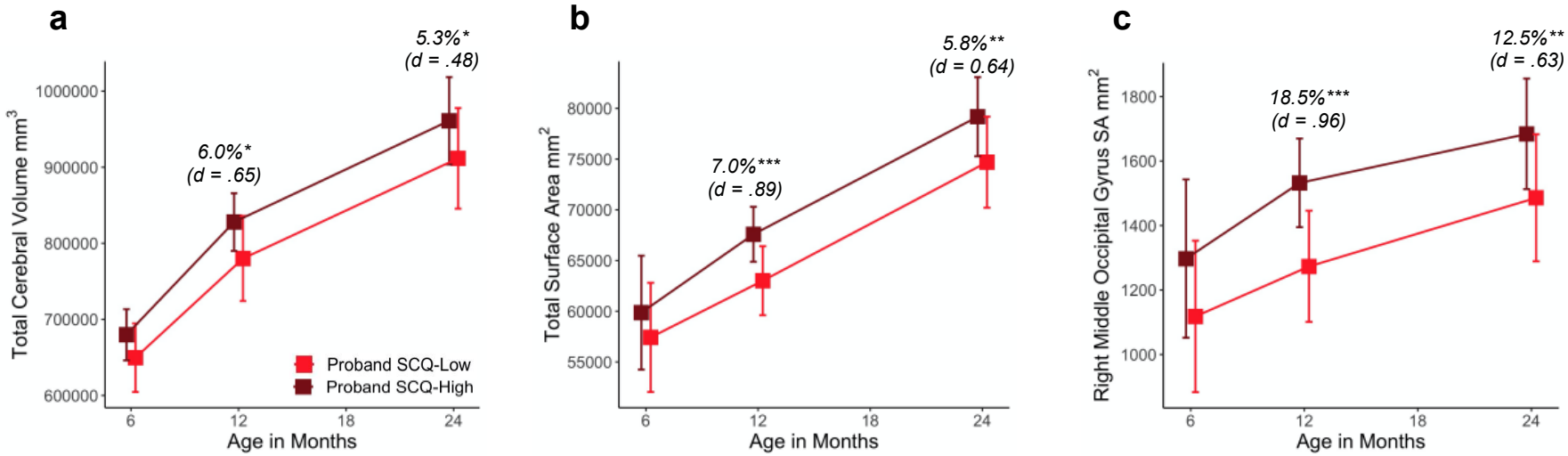

Least squares (LS) means of total cerebral volume, cortical surface area, and right middle occipital gyrus surface area (SA) are plotted at 6, 12, and 24 months for ASD siblings based on proband SCQ group (SCQ ≥ 21 = SCQ-High; SCQ < 21 = SCQ-Low). ASD siblings of probands with higher SCQ scores (SCQ-High) exhibited a 6.0% (Cohen's d = 0.65) and 5.3% (Cohen's d = 0.48) increase in model-adjusted total cerebral volume at 12 ($F_{1,33}$ = 4.88, P = 0.034) and 24 months of age ($F_{1,41}$ = 5.15, P = 0.029), respectively, compared to ASD siblings of probands with lower SCQ scores (SCQ-Low) (**a**). Similar increases were observed at 12 ($F_{1,33}$ = 15.11, P = 0.0005) and 24 months ($F_{1,40}$ = 7.80, P = 0.008) for total surface area (**b**). The greatest differences were observed in right middle occipital cortical surface area, with ASD siblings of SCQ-High probands exhibiting an 18.5% (Cohen's d = 0.96) and 12.5% (Cohen's d = 0.63) increase in regional surface area at 12 ($F_{1,33}$ = 14.89, P = 0.0005) and 24 months ($F_{1,40}$ = 7.77, P = 0.008), respectively (**c**). LS means are adjusted for proband and sibling age and sex. Percent differences between groups are reported where significant (*P < .05, **P < .01, ***P < .001) along with adjusted Cohen's d effect size estimates. Error bars represent 95% confidence intervals around LS means.

FIGURE S3. Scatterplots of Proband SCQ Versus Sibling Regional Surface Area

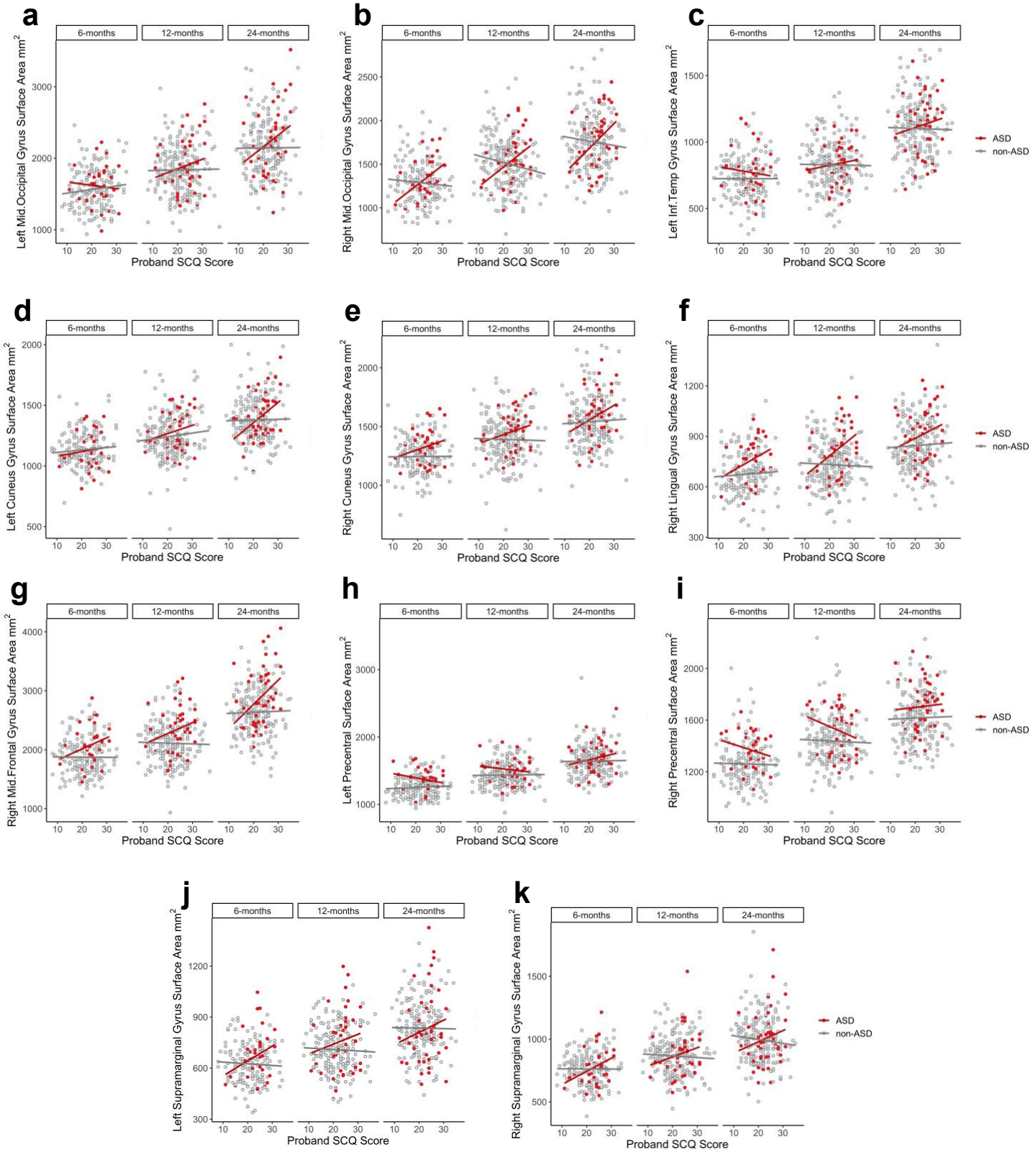

Scatterplots depicting bi-variate correlations between proband SCQ scores and sibling regional surface area measurements at 6, 12, and 24 months. Occipital regions of interest (a,b,d,e,f), additional hyper-expanding regions (c,g), and control regions (h-k) were investigated. Pearson correlation values by group and age are shown in Table S9. Visual depiction of correlations in brain space are depicted in Figure 2 in the main text.

TABLE S1. Sample Demographics (N = 384 proband-sibling pairs)

	Probands		**ASD Siblings**		**Non-ASD Siblings**		**Group Comparison**		
	n	%	n	%	n	%	X/t	df	p
Sex							14.46	1	<0.001[a]
Male (n,%)	331	86.2	69	77.5	160	54.2			
Female (n,%)	53	13.8	20	22.5	135	45.8			
Child Race									0.568[b]
Asian (n,%)			1	1.1	4	1.4			
Black (n,%)			2	2.2	10	3.4			
More than one race (n,%)			13	14.6	26	8.8			
White (n,%)			71	79.8	249	84.4			
Missing (n,%)			2	2.2	6	2.0			
Maternal Education									0.34[b]
Less than college (n,%)	126	32.8	26	40.4	90	30.5			
College degree (n,%)	145	37.8	27	30.3	118	40.0			
Graduate degree (n,%)	94	24.5	23	25.8	71	24.1			
Not answered (n,%)	4	1.0	0	0.0	4	1.4			
Missing (n,%)	7	1.8	2	2.2	5	1.7			
Autistic Traits	mean	SD	mean	SD	mean	SD			
Proband SCQ Score (mean, SD)	21.27	5.59	22.44	5.23	20.93	5.65	-2.20	134	0.029[a]
Sibling ADOS Severity Score (mean, SD)			5.86	1.88	1.61	0.99	-20.43	102	0.001[a]

[a]Testing for significant differences in distributions (Chi Square), or mean scores (t-tests) for ASD vs. non-ASD unless otherwise noted.
[b]Testing for significant differences in distributions using Fisher's Exact Test for ASD vs non-ASD due to small counts

TABLE S2. Count of Imaging Data Sets At Each Visit

	ASD	**Non-ASD**	***Total***
6 months			
sMRI	52	186	238
DTI	46	152	198
fcMRI	13	45	58
12 months			
sMRI	44	209	253
DTI	41	187	228
24 months			
sMRI	54	204	258
DTI	48	176	224
Total	298	1159	1457

TABLE S3. Correlations Between Infant Brain Phenotypes and Proband ASD Trait Level

	ASD					Non-ASD				
	n	r	95% CI	P value	*q* value	n	r	95% CI	P value	*q* value
TSA										
6 months	33	0.28	(-0.07, 0.57)	0.115	0.173	153	-0.02	(-0.18, 0.14)	0.8	0.845
12 months	39	0.40	(0.1, 0.64)	0.011	0.045	194	-0.08	(-0.22, 0.06)	0.246	0.845
24 months	46	0.41	(0.14, 0.63)	0.004	0.036	181	-0.04	(-0.18, 0.11)	0.633	0.845
TCV										
6 months	44	0.31	(0.02, 0.56)	0.039	0.070	167	-0.02	(-0.17, 0.14)	0.845	0.845
12 months	39	0.36	(0.05, 0.61)	0.024	0.054	194	-0.06	(-0.2, 0.08)	0.43	0.845
24 months	48	0.35	(0.07, 0.58)	0.015	0.045	186	-0.04	(-0.18, 0.11)	0.635	0.845
EA-CSF										
6 months	42	-0.02	(-0.32, 0.29)	0.905	0.905	149	-0.02	(-0.18, 0.14)	0.821	0.845
12 months	39	0.16	(-0.16, 0.46)	0.319	0.359	182	-0.07	(-0.21, 0.08)	0.370	0.845
24 months	42	0.20	(-0.11, 0.48)	0.202	0.260	159	-0.10	(-0.25, 0.06)	0.222	0.845

TABLE S4. Correlations Between Infant Brain Phenotypes and Proband ADI-R Scores

	ASD					Non-ASD				
	n	r	95% CI	P value	*q* value	n	r	95% CI	P value	*q* value
	Proband Reciprocal Social Interaction									
TSA										
6 months	35	0.12	(-0.23, 0.43)	0.506	0.506	164	-0.04	(-0.19, 0.11)	0.599	0.756
12 months	42	0.47	(0.19, 0.67)	0.002	0.012	205	-0.05	(-0.19, 0.08)	0.449	0.63
24 months	50	0.33	(0.05, 0.55)	0.021	0.032	194	-0.05	(-0.19, 0.09)	0.495	0.756
TCV										
6 months	47	0.13	(-0.17, 0.4)	0.4	0.48	181	-0.04	(-0.18, 0.11)	0.63	0.756
12 months	42	0.4	(0.11, 0.63)	0.008	0.024	206	-0.08	(-0.21, 0.06)	0.274	0.63
24 months	52	0.33	(0.06, 0.55)	0.016	0.032	200	-0.07	(-0.2, 0.07)	0.344	0.756
	Proband Restricted and Repetitive Behaviors									
TSA										
6 months	35	0	(-0.33, 0.33)	0.998	0.998	164	-0.11	(-0.26, 0.04)	0.154	0.185
12 months	42	0.17	(-0.14, 0.45)	0.283	0.849	205	-0.07	(-0.2, 0.07)	0.341	0.341
24 months	50	0.11	(-0.18, 0.37)	0.459	0.918	194	-0.13	(-0.26, 0.01)	0.077	0.115
TCV										
6 months	47	0.02	(-0.27, 0.3)	0.915	0.998	181	-0.17	(-0.3, -0.02)	0.025	0.115
12 months	42	0.25	(-0.06, 0.52)	0.108	0.648	205	-0.11	(-0.24, 0.03)	0.112	0.168
24 months	52	0.05	(-0.23, 0.32)	0.736	0.998	200	-0.15	(-0.28, -0.01)	0.039	0.115

TABLE S5. Longitudinal Models Predicting Sibling Cerebral Volume and Surface Area From Proband ADI-R Scores

	Estimate[a]	95% CI	df	P value
Proband Reciprocal Social Interaction				
Cerebral Volume				
Intercept	777940.31	(744283.11, 811597.51)	400	<0.001
Proband ADI-R RSI	-790.399	(-2316.62, 735.82)	316	0.309
Sibling Sex - Male	74767.5	(58857.28, 90677.72)	316	<0.001
Sibling Group - ASD	-69450.466	(-137454.91, -1446.02)	316	0.045
Group x Proband ADI-R RSI	4254.489	(953.17, 7555.81)	316	0.012
Group x Age MRI	348.287	(-777.79, 1474.37)	400	0.544
Site 2	-10932.997	(-33168.24, 11302.25)	316	0.334
Site 3	-13999.623	(-34643.26, 6644.02)	316	0.183
Site 4	5280.923	(-16446.94, 27008.79)	316	0.633
Sibling Age at MRI	6544.691	(6050.51, 7038.87)	400	<0.001
Surface Area				
Intercept	56969.744	(54871.26, 59068.23)	394	<0.001
Proband ADI-R RSI	-55.515	(-150.83, 39.8)	286	0.253
Sibling Sex - Male	4420.154	(3406.51, 5433.79)	286	<0.001
Sibling Group - ASD	-4154.553	(-8512.05, 202.94)	286	0.062
Group x Proband ADI-R RSI	261.752	(48.92, 474.58)	286	0.016
Group x Age MRI	13.098	(-38.63, 64.83)	394	0.619
Site 2	312.27	(-1130.57, 1755.11)	286	0.67
Site 3	-457.549	(-1801.99, 886.89)	286	0.503
Site 4	249.303	(-1153.5, 1652.11)	286	0.727
Sibling Age at MRI	1055.839	(1033.2, 1078.48)	394	<0.001
Proband Restricted and Repetitive Behavior				
Cerebral Volume				
Intercept	787837.842	(758121.78, 817553.9)	400	<0.001
Proband ADI-R RRB	-3512.415	(-6864.84, -159.99)	316	0.04
Sibling Sex - Male	75580.986	(59613.16, 91548.82)	316	<0.001
Sibling Group - ASD	-30043.183	(-82778.62, 22692.26)	316	0.263
Group x Proband ADI-R RRB	6973.762	(-819.06, 14766.59)	316	0.079
Group x Age MRI	291.789	(-832.65, 1416.22)	400	0.61
Site 2	-13240.078	(-35524.47, 9044.31)	316	0.243
Site 3	-15286.97	(-35761.77, 5187.83)	316	0.143
Site 4	-771.366	(-22939.1, 21396.37)	316	0.945
Sibling Age at MRI	6563.688	(6070.27, 7057.1)	400	<0.001
Surface Area				
Intercept	56708.523	(54833.17, 58583.88)	394	<0.001
Proband ADI-R RRB	-106.659	(-319, 105.68)	286	0.324
Sibling Sex - Male	4531.589	(3509.47, 5553.71)	286	<0.001
Sibling Group - ASD	-835.451	(-4301.89, 2630.99)	286	0.636
Group x Proband ADI-R RRB	283.38	(-226.14, 792.9)	286	0.275
Group x Age MRI	11.51	(-40.5, 63.52)	394	0.664
Site 2	175.335	(-1275.5, 1626.17)	286	0.812
Site 3	-624.571	(-1966.34, 717.2)	286	0.36
Site 4	-34.004	(-1470.13, 1402.12)	286	0.963
Sibling Age at MRI	1055.926	(1033.15, 1078.71)	394	<0.001

[a]Reference groups for sex and sibling diagnostic group are female and non-ASD, respectively.

TABLE S6. Linear Mixed Model Results for Total Cerebral Volume and Surface Area Controlling for Younger Sibling's ADOS Calibrated Severity Score

	Estimate	95% CI	df	P value
Cerebral Volume Model				
Intercept	752991.7	(729162, 776821.44)	368	<0.001
Proband SCQ	-974.033	(-2520.46, 572.39)	287	0.216
Sibling Sex - Male	74593.52	(57883.06, 91303.98)	287	<0.001
Sibling Group - ASD	-20519.9	(-57211.24, 16171.46)	287	0.272
Group x Proband SCQ	6310.207	(2464.03, 10156.38)	287	0.001
Group x Age MRI	273.427	(-895.18, 1442.04)	368	0.646
ADOS CSS (24 Months)	5701.471	(-951.05, 12353.99)	287	0.093
Site 2	-13665.8	(-37391.59, 10060.03)	287	0.258
Site 3	-8789.34	(-30542.83, 12964.15)	287	0.427
Site 4	4253.309	(-18955.03, 27461.65)	287	0.719
Sibling Age at MRI	6507.459	(5987.99, 7026.93)	368	<0.001
Surface Area Model				
Intercept	55315.7	(53824.63, 56806.78)	363	<0.001
Proband SCQ	-69.993	(-164.5, 24.52)	262	0.146
Sibling Sex - Male	4588.613	(3541.47, 5635.76)	262	<0.001
Sibling Group - ASD	-1337.5	(-3622.45, 947.45)	262	0.25
Group x Proband SCQ	385.244	(119.58, 650.91)	262	0.005
Group x Age MRI	8.085	(-46.9, 63.07)	363	0.773
ADOS CSS (24 Months)	384.316	(-43.18, 811.81)	262	0.078
Site 2	51.862	(-1444.71, 1548.43)	262	0.946
Site 3	-502.38	(-1886.32, 881.56)	262	0.475
Site 4	109.269	(-1355.16, 1573.7)	262	0.883
Sibling Age at MRI	1057.301	(1033.11, 1081.49)	363	<0.001

TABLE S7. Linear Mixed Model Results for Regional Brain Phenotypes Controlling for Younger Sibling's ADOS Calibrated Severity Score

	Estimate	95% CI	df	P value
Right Middle Frontal Gyrus				
Intercept	1701.723	(1584.22, 1819.22)	363	<0.001
Proband SCQ	-2.907	(-10.32, 4.51)	262	0.441
Sibling Sex - Male	196.737	(114.27, 279.21)	262	<0.001
Sibling Group - ASD	88.273	(-91.3, 267.84)	262	0.334
Group x Proband SCQ	18.939	(-1.85, 39.73)	262	0.074
Group x Age MRI	3.964	(-0.81, 8.74)	363	0.104
ADOS CSS (24 Months)	-1.941	(-35.42, 31.54)	262	0.909
Site 2	-10.257	(-128.09, 107.57)	262	0.864
Site 3	41.263	(-67.83, 150.35)	262	0.457
Site 4	26.804	(-88.56, 142.17)	262	0.648
Sibling Age at MRI	43.718	(41.63, 45.81)	363	<0.001
Left Cuneus				
Intercept	1095.73	(1039.75, 1151.71)	363	<0.001
Proband SCQ	1.955	(-1.58, 5.49)	262	0.278
Sibling Sex - Male	86.24	(46.93, 125.55)	262	<0.001
Sibling Group - ASD	0.97	(-84.5, 86.43)	262	0.982
Group x Proband SCQ	6.619	(-3.29, 16.52)	262	0.189
Group x Age MRI	0.405	(-1.55, 2.36)	363	0.684
ADOS CSS (24 Months)	-5.692	(-21.67, 10.28)	262	0.484
Site 2	26.369	(-29.84, 82.57)	262	0.356
Site 3	-11.16	(-63.17, 40.85)	262	0.673
Site 4	13.319	(-41.71, 68.35)	262	0.634
Sibling Age at MRI	13.264	(12.41, 14.12)	363	<0.001
Right Lingual Gyrus				
Intercept	634.155	(586.89, 681.42)	363	<0.001
Proband SCQ	-0.695	(-3.68, 2.29)	262	0.647
Sibling Sex - Male	57.235	(24.11, 90.36)	262	<0.001
Sibling Group - ASD	36.509	(-35.9, 108.91)	262	0.322
Group x Proband SCQ	10.842	(2.5, 19.18)	262	0.011
Group x Age MRI	-0.605	(-2.4, 1.19)	363	0.507
ADOS CSS (24 Months)	4.49	(-8.95, 17.93)	262	0.511
Site 2	-0.823	(-48.17, 46.53)	262	0.973
Site 3	10.376	(-33.43, 54.18)	262	0.641
Site 4	12.593	(-33.75, 58.93)	262	0.593
Sibling Age at MRI	8.67	(7.89, 9.45)	363	<0.001
Right Middle Occipital Gyrus				
Intercept	1215.897	(1127.32, 1304.47)	363	<0.001
Proband SCQ	-6.359	(-11.96, -0.76)	262	0.026
Sibling Sex - Male	143.353	(81.16, 205.54)	262	<0.001
Sibling Group - ASD	-73.421	(-208.96, 62.12)	262	0.287
Group x Proband SCQ	26.69	(10.94, 42.44)	262	<0.001
Group x Age MRI	0.12	(-3.26, 3.5)	363	0.945
ADOS CSS (24 Months)	3.764	(-21.6, 29.13)	262	0.77
Site 2	7.244	(-81.63, 96.12)	262	0.873

Site 3	-9.044	(-91.3, 73.22)	262	0.829
Site 4	-11.659	(-98.72, 75.41)	262	0.792
Sibling Age at MRI	25.2	(23.71, 26.69)	363	<0.001

TABLE S8. Linear Mixed Model Results Including Time Interaction Term for Splenium FA Controlling for Younger Sibling's ADOS Calibrated Severity Score

	Estimate	95% CI	df	P value
CC Splenium				
Intercept	0.46643	(0.4554, 0.47746)	291	<0.001
Proband SCQ	0.00016	(-0.00069, 0.00101)	275	0.708
Sibling Sex - Male	0.00434	(-0.00336, 0.01203)	275	0.268
Sibling Group - ASD	-0.01536	(-0.03318, 0.00246)	275	0.091
Group x Proband SCQ	0.00174	(-0.00038, 0.00386)	275	0.107
Group x Age MRI	0.00023	(-0.00054, 0.00099)	291	0.563
Proband SCQ x Age MRI	0.00003	(-0.00003, 0.00009)	291	0.32
Group x SCQ x Age MRI	-0.00014	(-0.00029, 0)	291	0.058
ADOS CSS (24 Months)	0.00103	(-0.00202, 0.00408)	275	0.508
Site - 2	-0.00044	(-0.01146, 0.01057)	275	0.937
Site - 3	-0.01733	(-0.02725, -0.00742)	275	<0.001
Site - 4	0.00148	(-0.00889, 0.01184)	275	0.779
Sibling Age at MRI	0.00415	(0.00383, 0.00447)	291	<0.001

TABLE S9. Correlations Between Regional Infant Brain Phenotypes and Proband ASD Trait Level

	ASD					**Non-ASD**				
	n	r	95% CI	P	*q*	n	r	95% CI	P	*q*
Left Precentral Gyrus (Control ROI)										
6 months	33	-0.2	(-0.51, 0.15)	0.263	0.413	153	0.06	(-0.1, 0.22)	0.466	1
12 months	39	-0.12	(-0.42, 0.2)	0.458	0.568	194	0.02	(-0.13, 0.16)	0.826	1
24 months	46	0.18	(-0.12, 0.44)	0.244	0.41	181	0.01	(-0.13, 0.16)	0.854	1
Right Precentral Gyrus (Control ROI)										
6 months	33	-0.2	(-0.51, 0.16)	0.274	0.413	153	-0.02	(-0.18, 0.14)	0.827	1
12 months	39	-0.23	(-0.51, 0.09)	0.153	0.36	194	-0.03	(-0.17, 0.11)	0.659	1
24 months	46	0.05	(-0.24, 0.34)	0.729	0.765	181	0.02	(-0.12, 0.17)	0.765	1
Right Middle Frontal Gyrus										
6 months	33	0.26	(-0.09, 0.55)	0.146	0.36	153	-0.01	(-0.17, 0.15)	0.931	1
12 months	39	0.23	(-0.09, 0.51)	0.163	0.36	194	-0.02	(-0.16, 0.12)	0.748	1
24 months	46	0.38	(0.1, 0.6)	0.01	0.084	181	0.02	(-0.12, 0.17)	0.743	1
Left Cuneus										
6 months	33	0.11	(-0.24, 0.44)	0.542	0.65	153	0.08	(-0.08, 0.24)	0.328	1
12 months	39	0.2	(-0.12, 0.49)	0.216	0.405	194	0.11	(-0.04, 0.24)	0.141	1
24 months	46	0.4	(0.12, 0.62)	0.006	0.084	181	0.02	(-0.13, 0.16)	0.831	1
Right Cuneus										
6 months	33	0.22	(-0.14, 0.52)	0.222	0.405	153	0.01	(-0.15, 0.17)	0.929	1
12 months	39	0.22	(-0.1, 0.5)	0.173	0.363	194	-0.02	(-0.16, 0.12)	0.766	1
24 months	46	0.27	(-0.02, 0.52)	0.069	0.266	181	0.04	(-0.11, 0.18)	0.605	1
Right Lingual Gyrus										
6 months	33	0.3	(-0.04, 0.59)	0.086	0.278	153	0.06	(-0.1, 0.21)	0.491	1
12 months	39	0.38	(0.07, 0.62)	0.017	0.102	194	-0.03	(-0.17, 0.11)	0.633	1
24 months	46	0.21	(-0.08, 0.47)	0.159	0.36	181	0.04	(-0.11, 0.19)	0.58	1
Left Middle Occipital Gyrus										
6 months	33	-0.07	(-0.41, 0.28)	0.683	0.736	153	0.1	(-0.06, 0.26)	0.212	1
12 months	39	0.18	(-0.14, 0.47)	0.275	0.413	194	0.01	(-0.13, 0.15)	0.857	1
24 months	46	0.26	(-0.03, 0.52)	0.076	0.266	181	0.01	(-0.14, 0.15)	0.936	1

Right Middle Occipital Gyrus										
6 months	33	0.44	(0.11, 0.68)	0.01	0.084	153	-0.07	(-0.23, 0.09)	0.373	1
12 months	39	0.38	(0.07, 0.62)	0.017	0.102	194	-0.16	(-0.3, -0.02)	0.024	1
24 months	46	0.39	(0.11, 0.61)	0.007	0.084	181	-0.08	(-0.22, 0.06)	0.274	1
Left Supramarginal gyrus (Control ROI)										
6 months	33	0.27	(-0.08, 0.56)	0.133	0.36	153	-0.05	(-0.21, 0.11)	0.546	1
12 months	39	0.16	(-0.16, 0.45)	0.329	0.461	194	-0.04	(-0.18, 0.1)	0.594	1
24 months	46	0.15	(-0.15, 0.42)	0.316	0.458	181	-0.01	(-0.16, 0.13)	0.882	1
Right Supramarginal gyrus (Control ROI)										
6 months	33	0.32	(-0.03, 0.6)	0.07	0.266	153	0	(-0.16, 0.15)	0.961	1
12 months	39	0.19	(-0.13, 0.48)	0.239	0.41	194	-0.05	(-0.19, 0.09)	0.486	1
24 months	46	0.19	(-0.1, 0.46)	0.2	0.4	181	-0.09	(-0.23, 0.06)	0.239	1
Left inferior temporal gyrus										
6 months	33	-0.08	(-0.41, 0.27)	0.644	0.712	153	0	(-0.16, 0.16)	1	1
12 months	39	0.12	(-0.2, 0.42)	0.46	0.568	194	-0.01	(-0.15, 0.13)	0.869	1
24 months	46	0.13	(-0.17, 0.4)	0.402	0.528	181	-0.02	(-0.16, 0.13)	0.832	1
CC Splenium										
6 months	42	0.45	(0.17, 0.66)	0.003	0.084	137	-0.02	(-0.19, 0.15)	0.826	1
12 months	36	-0.09	(-0.4, 0.25)	0.616	0.699	172	0.03	(-0.12, 0.18)	0.657	1
24 months	40	0.09	(-0.23, 0.39)	0.581	0.678	160	0.04	(-0.12, 0.19)	0.637	1
CC Genu										
6 months	42	0.29	(-0.01, 0.55)	0.059	0.266	137	0	(-0.16, 0.17)	0.959	1
12 months	36	0.15	(-0.19, 0.45)	0.387	0.524	172	0.06	(-0.09, 0.2)	0.468	1
24 months	40	0.27	(-0.05, 0.53)	0.096	0.288	159	0.08	(-0.07, 0.23)	0.302	1
CC Body										
6 months	42	0.29	(-0.01, 0.55)	0.06	0.266	137	0	(-0.17, 0.17)	0.999	1
12 months	36	0.05	(-0.29, 0.37)	0.789	0.789	172	0.02	(-0.13, 0.16)	0.842	1
24 months	40	0.05	(-0.26, 0.36)	0.754	0.772	160	0	(-0.16, 0.15)	0.982	1

TABLE S10. Linear Mixed Model Results for Regional Brain Phenotypes

	Estimate	95% CI	df	P value[a]
Right Middle Frontal Gyrus				
Intercept	1697.077	(1598.56, 1795.59)	369	<0.001
Proband SCQ	-2.857	(-10.2, 4.49)	267	0.444
Sibling Sex - Male	198.675	(117.6, 279.75)	267	<0.001
Sibling Group - ASD	81.229	(-28.22, 190.68)	267	0.145
Group x Proband SCQ	18.777	(-1.84, 39.39)	267	0.074
Group x Age at MRI	4.029	(-0.71, 8.77)	369	0.096
Site - 2	-9.572	(-125.88, 106.73)	267	0.871
Site - 3	36.647	(-70.3, 143.6)	267	0.5
Site - 4	27.212	(-86.95, 141.37)	267	0.639
Sibling Age at MRI	43.653	(41.59, 45.71)	369	<0.001
Left Cuneus				
Intercept	1087.363	(1040.21, 1134.52)	369	<0.001
Proband SCQ	1.905	(-1.62, 5.43)	267	0.288
Sibling Sex - Male	83.145	(44.29, 122)	267	<0.001
Sibling Group - ASD	-21.744	(-73.65, 30.17)	267	0.41
Group x Proband SCQ	6.674	(-3.2, 16.55)	267	0.184
Group x Age at MRI	0.391	(-1.56, 2.34)	369	0.693
Site - 2	27.956	(-27.82, 83.73)	267	0.325
Site - 3	-11.46	(-62.73, 39.81)	267	0.66
Site - 4	14.398	(-40.35, 69.14)	267	0.605
Sibling Age at MRI	13.284	(12.44, 14.13)	369	<0.001
Right Lingual Gyrus				
Intercept	641.904	(601.98, 681.83)	369	<0.001
Proband SCQ	-0.77	(-3.74, 2.2)	267	0.611
Sibling Sex - Male	57.514	(24.72, 90.31)	267	<0.001
Sibling Group - ASD	56.097	(11.37, 100.82)	267	0.014
Group x Proband SCQ	10.882	(2.56, 19.21)	267	0.011
Group x Age at MRI	-0.613	(-2.39, 1.17)	369	0.499
Site - 2	-2.645	(-49.71, 44.42)	267	0.912
Site - 3	7.27	(-35.98, 50.52)	267	0.741
Site - 4	11.939	(-34.24, 58.12)	267	0.611
Sibling Age at MRI	8.682	(7.91, 9.45)	369	<0.001
Right Middle Occipital Gyrus				
Intercept	1226.628	(1152.15, 1301.1)	369	<0.001
Proband SCQ	-6.369	(-11.94, -0.8)	267	0.025
Sibling Sex - Male	137.273	(75.91, 198.63)	267	<0.001
Sibling Group - ASD	-56.767	(-138.19, 24.66)	267	0.171
Group x Proband SCQ	26.821	(11.15, 42.5)	267	<0.001
Group x Age at MRI	0.143	(-3.21, 3.5)	369	0.933
Site - 2	5.894	(-82.17, 93.95)	267	0.895
Site - 3	-8.002	(-88.95, 72.95)	267	0.846
Site - 4	-13.116	(-99.56, 73.33)	267	0.765
Sibling Age at MRI	25.161	(23.69, 26.63)	369	<0.001

[a]Bonferroni correction applied to the Group x Proband SCQ effect of interest
* = p-values < 0.01(0.05/5).

TABLE S11. Linear Mixed Model Results Including Time Interaction Term for Splenium FA

	Estimate	95% CI	df	P value
CC Splenium				
Intercept	0.46852	(0.45923, 0.47781)	295	<0.001
Proband SCQ	0.00015	(-0.0007, 0.001)	280	0.734
Sibling Sex - Male	0.00426	(-0.00337, 0.01188)	280	0.273
Sibling Group - ASD	-0.01093	(-0.02251, 0.00066)	280	0.064
Group x Proband SCQ	0.00172	(-0.0004, 0.00383)	280	0.111
Group x Age MRI	0.00023	(-0.00053, 0.00099)	295	0.55
Proband SCQ x Age MRI	0.00003	(-0.00005, 0.00008)	295	0.35
Group x SCQ x Age MRI	-0.00014	(-0.00029, 0.00001)	295	0.062
Site - 2	-0.00092	(-0.01184, 0.01001)	280	0.869
Site - 3	-0.01767	(-0.02744, -0.0079)	280	<0.001
Site - 4	0.00114	(-0.00917, 0.01145)	280	0.828
Sibling Age at MRI	0.00414	(0.00382, 0.00445)	295	<0.001

TABLE S12. fcMRI Enrichment Results Table

Network 1	**Network 2**	**SCQ P-value**	**ADI-R P-value**	**Vineland Soc P-value**
pDMN	VIS		0.0097	0.0012
pDMN	mVIS			0.0094
pDMN	SM1		0.0031	
pFP	VIS	0.0077		

REFERENCES

1. Hazlett HC, Gu H, Munsell BC, et al.: Early brain development in infants at high risk for autism spectrum disorder. Nature 2017; 542:348–351

2. Hazlett HC, Gu H, McKinstry RC, et al.: Brain volume findings in 6-month-old infants at high familial risk for autism. The American journal of psychiatry 2012; 169:601–608

3. Wang JY, Hagerman RJ, Rivera SM: A multimodal imaging analysis of subcortical gray matter in fragile X premutation carriers. Mov Disord Official J Mov Disord Soc 2013; 28:1278–84

4. Tzourio-Mazoyer N, Landeau B, Papathanassiou D, et al.: Automated anatomical labeling of activations in SPM using a macroscopic anatomical parcellation of the MNI MRI single-subject brain. NeuroImage 2002; 15:273–289

5. Kim SH, Fonov VS, Dietrich C, et al.: Adaptive prior probability and spatial temporal intensity change estimation for segmentation of the one-year-old human brain. J Neurosci Meth 2012; 212:43–55

6. Shen MD, Kim SH, McKinstry RC, et al.: Increased Extra-axial Cerebrospinal Fluid in High-Risk Infants Who Later Develop Autism. Biological psychiatry 2017; 82:186–193

7. Sled JG, Zijdenbos AP, Evans AC: A nonparametric method for automatic correction of intensity nonuniformity in MRI data. Ieee T Med Imaging 2020; 17:87–97

8. Collins DL, Neelin P, Peters TM, et al.: Automatic 3D Intersubject Registration of MR Volumetric Data in Standardized Talairach Space. J Comput Assist Tomo 1994; 18:192–205

9. Smith SM: Fast robust automated brain extraction. Human brain mapping 2002; 17:143–155

10. Gouttard S, Styner M, Joshi S, et al.: Subcortical structure segmentation using probabilistic atlas priors2007; 65122J

11. Oguz I, Farzinfar M, Matsui J, et al.: DTIPrep: quality control of diffusion-weighted images. Frontiers in neuroinformatics 2014; 8:4

12. Wolff JJ, Swanson MR, Elison JT, et al.: Neural circuitry at age 6 months associated with later repetitive behavior and sensory responsiveness in autism. Molecular autism 2017; 8:8

13. Verde AR, Budin F, Berger J-B, et al.: UNC-Utah NA-MIC framework for DTI fiber tract analysis. Frontiers in neuroinformatics 2014; 7:51

14. Eggebrecht AT, Elison JT, Feczko E, et al.: Joint Attention and Brain Functional Connectivity in Infants and Toddlers. Cerebral cortex (New York, NY : 1991) 2017; 27:1709–1720

15. Emerson RW, Gao W, Lin W: Longitudinal Study of the Emerging Functional Connectivity Asymmetry of Primary Language Regions during Infancy. The Journal of neuroscience : the official journal of the Society for Neuroscience 2016; 36:10883–10892

16. Ojemann JG, Akbudak E, Snyder AZ, et al.: Anatomic Localization and Quantitative Analysis of Gradient Refocused Echo-Planar fMRI Susceptibility Artifacts. NeuroImage 1997; 6:156–167

17. Power JD, Mitra A, Laumann TO, et al.: Methods to detect, characterize, and remove motion artifact in resting state fMRI. NeuroImage 2014; 84:320–341

18. Nielsen AN, Greene DJ, Gratton C, et al.: Evaluating the Prediction of Brain Maturity From Functional Connectivity After Motion Artifact Denoising. Cereb Cortex 2018; 29:2455–2469

19. Pruett JR, Kandala S, Hoertel S, et al.: Accurate age classification of 6 and 12 month-old infants based on resting-state functional connectivity magnetic resonance imaging data. Developmental cognitive neuroscience 2015; 12:123–133

20. Dosenbach NUF, Fair DA, Miezin FM, et al.: Distinct brain networks for adaptive and stable task control in humans. Proc National Acad Sci 2007; 104:11073–11078

21. Marek S, Dosenbach NUF: The frontoparietal network: function, electrophysiology, and importance of individual precision mapping. Dialogues Clin Neurosci 2018; 20:133–140

22. Nair A, Jolliffe M, Lograsso YSS, et al.: A Review of Default Mode Network Connectivity and Its Association With Social Cognition in Adolescents With Autism Spectrum Disorder and Early-Onset Psychosis. Frontiers Psychiatry 2020; 11:614

23. Rosvall M, Bergstrom CT: Maps of random walks on complex networks reveal community structure. Proc National Acad Sci 2008; 105:1118–1123

24. Seitzman BA, Gratton C, Marek S, et al.: A set of functionally-defined brain regions with improved representation of the subcortex and cerebellum. Neuroimage 2020; 206:116290

25. Benjamini Y, Hochberg Y: Controlling the false discovery rate: a practical and powerful approach to multiple testing [Internet]. Journal of the Royal Statistical Society 1995; 57:289–300Available from: http://www.jstor.org/stable/2346101

26. Verbeke G, Verbeke G, Molenberghs G: Linear Mixed Models for Longitudinal Data [Internet]New York, NY, Springer New York, 1997, pp 63–153.Available from: https://doi.org/10.1007/978-1-4612-2294-1_3

27. Fitzmaurice GM, Laird NM, Ware JH: Applied Longitudinal Analysis. Wiley Ser Probab Statistics 2018; 441–472

28. Girault JB, Swanson MR, Meera SS, et al.: Quantitative trait variation in ASD probands and toddler sibling outcomes at 24 months. Journal of neurodevelopmental disorders 2020; 12:5

29. Rutter M, Couteur AL, Lord C: Autism diagnostic interview-revised. Western Psychological Services, 2003

30. Rolison M, Lacadie C, Chawarska K, et al.: Atypical Intrinsic Hemispheric Interaction Associated with Autism Spectrum Disorder Is Present within the First Year of Life. Cereb Cortex New York N Y 1991 2021;

31. Marrus N, Eggebrecht AT, Todorov A, et al.: Walking, Gross Motor Development, and Brain Functional Connectivity in Infants and Toddlers. Cerebral Cortex 2018; 28:750–763